

PAHs increase the production of extracellular vesicles both in vitro in endothelial cells and in vivo in urines from rats

Manon Le Goff, Dominique Lagadic-Gossmann, Remi Latour, Normand Podechard, Nathalie Grova, Fabienne Gauffre, Soizic Chevance, Agnès Burel, Brice M.R. Appenzeller, Lionel Ulmann, et al.

▶ **To cite this version:**

Manon Le Goff, Dominique Lagadic-Gossmann, Remi Latour, Normand Podechard, Nathalie Grova, et al.. PAHs increase the production of extracellular vesicles both in vitro in endothelial cells and in vivo in urines from rats. Environmental Pollution, 2019, 255, pp.113171. 10.1016/j.envpol.2019.113171 . hal-02302334

HAL Id: hal-02302334

https://univ-lemans.hal.science/hal-02302334

Submitted on 20 Jul 2022

HAL is a multi-disciplinary open access archive for the deposit and dissemination of scientific research documents, whether they are published or not. The documents may come from teaching and research institutions in France or abroad, or from public or private research centers.

L'archive ouverte pluridisciplinaire **HAL**, est destinée au dépôt et à la diffusion de documents scientifiques de niveau recherche, publiés ou non, émanant des établissements d'enseignement et de recherche français ou étrangers, des laboratoires publics ou privés.



Distributed under a Creative Commons Attribution - NonCommercial 4.0 International License

Version of Record: https://www.sciencedirect.com/science/article/pii/S0269749119331136
Manuscript_7777229f3e14dfd732837f3c11d21e9b

PAHs increase the production of extracellular vesicles both *in vitro* in endothelial cells and *in vivo* in urines from rats

Manon Le Goff[1,2], Dominique Lagadic-Gossmann[1], Remi Latour[1], Normand Podechard[1], Nathalie Grova[5,6], Fabienne Gauffre[3], Soizic Chevance[3], Agnès Burel[4], Brice M. R. Appenzeller[7], Lionel Ulmann[2], Odile Sergent[1] and Eric Le Ferrec[1]*

[1] Univ Rennes, Inserm, EHESP, Irset (Institut de recherche en santé environnement et travail) – UMR_S 1085, F-35000 Rennes, France
[2] EA 2160 Mer Molécules Santé – MIMMA, IUML FR-3473 CNRS, Le Mans Université, Laval F-53020, France
[3] Univ Rennes, CNRS, ISCR (Institut des Sciences Chimiques de Rennes) – UMR_6226, F-35000 Rennes, France
[4] Univ Rennes, Biosit – UMS 3480, US_S 018, F-35000 Rennes, France
[5]Immune Endocrine Epigenetics Research Group, Department of Infection and Immunity-Luxembourg Institute of Health, 29 rue Henri Koch, L-4354, Esch-sur-Alzette, Grand Duchy of Luxembourg
[6] Calbinotox, Faculty of Science and Technology-Lorraine University, Campus Aiguillettes, B.P. 70239, F-54506 Vandoeuvre-lès-Nancy, France
[7] Human Biomonitoring Research Unit, Luxembourg Institute of Health, 1 A-B Thomas Edisson, Grand Duchy of Luxembourg.

*** Corresponding author:**

Eric Le Ferrec, eric.leferrec@univ-rennes1.fr ; UMR Inserm U1085 / IRSET, University of Rennes 1, Faculty of Pharmacy, 2 av. Pr. Léon Bernard, 35043 RENNES cedex, France

Abbreviations:

AhR: aryl hydrocarbon receptor, AM: acetoxymethyl ester, Annexin V-PE: Annexin V-phycoerythrin, ARNT: aryl hydrocarbon receptor nuclear translocator, B[a]A: benz[*a*]anthracene, B[a]P: benzo[*a*]pyrene, B[e]P: benzo[*e*]pyrene, $[Ca^{2+}]_i$: intracellular calcium concentration, CVD: cardiovascular diseases, CYP: cytochrome, DBA: dibenz[*a,h*]anthracene, DMSO: dimethyl sulfoxide, DTT: dithiothreitol, EVs: extracellular vesicles, FBS: fetal bovine serum, HMEC-1: Human microvascular endothelial cell-line 1, L-EVs: large extracellular vesicles, MVB: multivesicular bodies, NTA: nanoparticle tracking analysis, PAHs: polycyclic aromatic hydrocarbons, PBS: phosphate-buffered saline, PFA: paraformaldehyde, PYR: pyrene, RT-PCR: real-time quantitative PCR, SDS-PAGE: sodium dodecyl sulfate–polymerase gel electrophoresis, S-EVs: small extracellular vesicles, TEM: transmission electron microscopy, uEVs: urinary EVs, US-EPA: United States Environmental Protection Agency, WHO: World Health Organization, XREs: xenobiotic responsive elements, α-NF: alpha-naphthoflavone.

© 2019 published by Elsevier. This manuscript is made available under the CC BY NC user license
https://creativecommons.org/licenses/by-nc/4.0/

Abstract (300 words)

Environmental contaminants, to which humans are widely exposed, cause or worsen several diseases, like cardiovascular diseases and cancers. Among these molecules, polycyclic aromatic hydrocarbons (PAHs) stand out since they are ubiquitous pollutants found in ambient air and diet. Because of their toxic effects, public Health agencies promote development of research studies aiming at increasing the knowledge about PAHs and the discovery of biomarkers of exposure and/or effects.

Extracellular vesicles (EVs), including small extracellular vesicles (S-EVs or exosomes) and large extracellular vesicles (L-EVs or microvesicles), are delivery systems for multimolecular messages related to the nature and status of the originating cells. Because they are produced by all cells and detected within body fluids, EV releases could act as cell responses and thereby serve as biomarkers. To test whether EVs can serve as biomarkers of PAHs exposure, we evaluate the effects of these pollutants on EV production using an *in vitro* approach (human endothelial cell line, HMEC-1) and an *in vivo* approach (urine samples from PAHs-exposed rats). Our study indicates that, i) PAH exposure increases *in vitro* the EV production by endothelial cells and *in vivo* the release of EVs in urine, and that the stimulating effects of PAHs concern both S-EVs and L-EVs; ii) PAH exposure and more particularly exposure to B[a]P, can influence the composition of exosomes produced by endothelial cells; iii) the aryl hydrocarbon receptor, a cytosolic receptor associated to most deleterious effects of PAHs, would be involved in the PAH effects on the release of S-EVs, but not L-EVs.

These results suggest that EVs may have utility for monitoring exposure to PAHs, and more particularly to B[a]P, considered as reference PAH, and to detect the related early cellular response prior to end-organ damages.

Capsule :

Exposure to polycyclic aromatic hydrocarbons, like benzo[a]pyrene, increases, *in-vitro* and *in-vivo*, production of exosomes and microvesicles and modifies their compositions

Keywords :

Polycyclic aromatic hydrocarbons, Aryl hydrocarbon receptor, Endothelial cells, Urine, Extracellular vesicles, Exosomes, Microvesicles, Large EVs, Small EVs

Highlights

- B[a]P stimulates EV production by endothelial HMEC-1 cells.
- B[a]P stimulates production of both S-EVs (exosomes)and L-EVs (microvesicles).
- B[a]P modifies protein cargoes of S-EVs.
- S-EV, but not L-EV, increased production by B[a]P is AhR dependent.
- *In vivo* exposure to PAHs increases urinary EV amount.

1. Introduction

Nowadays, there is broad consensus regarding the fact that our environmental health markedly depends on the impact of environmental contaminants to which humans are widely exposed[1], especially *via* diet and ambient air. Most of these chemicals, such as heavy metals, persistent organic pollutants and biocides, come from anthropogenic activities. They are known to cause or worsen several diseases, like cardiovascular diseases (CVD), immune dysfunctions and cancers[2]. Among these molecules, polycyclic aromatic hydrocarbons (PAHs) stand out since they are ubiquitous pollutants notably found in ambient air and diet. They are involved in the occurrence of human CVDs, and exhibit immunotoxic, mutagenic, and carcinogenic properties[3]. Most deleterious effects of PAHs are related to their binding to the aryl hydrocarbon receptor (AhR), a cytosolic ligand-activated transcription factor. PAH binding to this receptor triggers a canonical genomic pathway with the nuclear translocation of AhR followed by its interaction with aryl hydrocarbon receptor nuclear translocator (ARNT), thus allowing its binding to specific genomic elements termed xenobiotic responsive elements (XREs). XREs are found in the promoter of PAHs-responsive genes, such as cytochromes P-450 (CYP) 1A1 and 1B1, that are known carcinogen bioactivating enzymes. AhR activation also triggers several non-genomic pathways, including intracellular calcium signaling and tyrosine kinase SRC activation[4,5]. The United States Environmental Protection Agency (US-EPA) as well as the World Health Organization (WHO) consider some of PAHs as priority pollutants due to their critical effects on human health[6]. This has led to the development of research studies aiming at increasing the knowledge about these molecules and the discovery of biomarkers of exposure and/or effects.

During the last decade, extracellular vesicles (EVs) have drawn an increasing attention in the field of biomarkers of diseases or exposure to xenobiotics[7–11]. Theoretically produced by all cells, EVs, including small extracellular vesicles (S-EVs or exosomes) and large extracellular vesicles (L-EVs or microvesicles), are delivery systems for multimolecular messages closely related to the nature

and status of originating cells[12,13]. These cellular nanostructures are differentiated by their size (S-EV: less than 200 nm, L-EV: less than 1000 nm), their biogenesis processes (S-EV: generated within endosomal compartments , L-EV: budding from the plasma membrane) and by their components (lipids, proteins, DNAs, mRNAs, miRNAs...)[14]. EVs allow intercellular communication and consequently are involved in many biological processes such as cell maintenance and proliferation, tissue repair, angiogenesis... They have been detected within body fluids (i.e. blood, urine, lymph, saliva...) in healthy humans but also in patients[15,16]. In this latter case, EV production is exacerbated and their content altered. Such alterations notably occur during cancer, metabolic, neurodegenerative or CVDs[17,18] .

The EV overproduction is also observed during exposure to xenobiotics. Thus, some drugs or toxicants (like acetaminophen, alcohol, diclofenac or cigarette smoke) are able to increase *in vitro* and/or *in vivo* EV production, and to change their composition[19–22]. As a consequence, EVs could serve as biological markers of cell responses and possibly even susceptibility to toxicity. They also offer the possibility of detecting toxicity at the very early stages of development before irreversible effects occur.

Although the molecular mechanisms still remain to be fully clarified, there is evidence showing that an increase in intracellular calcium concentration ($[Ca^{2+}]_i$), plasma membrane remodeling or oxidative stress are involved in the EV release by cells[23,24]. Interestingly, we previously reported that PAHs and more specifically the prototypical PAH, benzo[a]pyrene (B[a]P), can trigger such cellular events. Indeed, our team previously demonstrated that cell exposure to various PAHs can increase the $[Ca^{2+}]_i$, *via* an AhR-independent activation of the β2-adrenergic receptor[25], and that membrane remodeling (characterized by an increase in fluidity and destabilization of lipid rafts), is a key mechanism in the B[a]P-associated toxicity[26].

Exposures to xenobiotics or lifestyle factors, such as air pollutants[27] cigarette smoke[28], alcohol[19], or high fat diet[29], would be able to modify EV trafficking, the amount produced and

composition (e.g. proteins, miRNA), notably in biological fluids such as plasma or urine. In this context, circulating EVs might provide information about both exposure level and toxic responses of the organism. EVs in blood plasma of healthy humans mainly originate from platelets. Comparatively, endothelial cells produce few EVs[30]. However, while the level of EV production by these latter cells is low under physiological conditions, it can considerably increase in pathological situation[30]. Thus, the amount of endothelium-derived EVs circulating in the blood stream has been shown to correlate with the severity of diverse diseases, eg. sepsis, stroke, atherosclerosis and metabolic syndrome [17]. Endothelial cells are also particularly interesting to focus on since they also participate in the production of EVs detected in urine[31,32]. It is within this framework that our study was carried out.

In order to test whether EVs can serve as biomarkers of PAH exposure, the present study was designed to evaluate the effects of these pollutants on EV production. To this aim, two different approaches were applied: i) an *in vitro* approach, using the human endothelial cell line HMEC-1; and ii) an *in vivo* approach, using urine samples obtained from PAH-exposed rats. Urine provides a good alternative to blood in the field of disease biomarkers because this biological fluid can be collected noninvasively and in large amounts[33]. Our present data demonstrate that PAHs can increase EV production by endothelial cells. This overproduction observed *in vitro* concerns both S-EVs and L-EVs probably involving different molecular mechanisms. Indeed, it seems that only the increase of S-EVs would be AhR-dependent. Moreover, the PAH-related increase in EV production was also observed *in vivo* in urine samples from rats exposed to the 16 PAHs listed as “priority” compounds by US-EPA.

2. Materials and Methods

2.1. *Chemicals and Reagents*

Benzo[*e*]pyrene (B[e]P), pyrene (PYR), benz[*a*]anthracene (B[a]A), benzo[*a*]pyrene (B[a]P), dibenz[*a,h*]anthracene (DBA), chrysene, benzo[b]fluoranthene, benzo[k]fluoranthene, benzo[g,h,i]perylene, indeno[1,2,3-c,d]pyrene, naphthalene, fluorene, acenaphthene, acenaphtylene, anthracene, phenanthrene, fluoranthene, alpha-naphthoflavone (α-NF), dimethyl sulfoxide (DMSO) and monoclonal antibody anti-β-actin were obtained from Sigma-Aldrich (St. Louis, MO, USA). Antibodies against CD63, lamin A/C and Hsc70 were from Santa Cruz Biotechnology (Santa Cruz, CA, USA), whereas Tsg101 was provided by Abcam and caveolin-1 and flotillin-1 by BD biosciences. All other chemicals used in this study were purchased from commercial sources at the highest purity available.

2.2. *Cell Culture*

The Human Microvascular Endothelial Cell line (HMEC-1) was obtained from the Center for Disease Control and Prevention (Atlanta, GA). Cells were routinely maintained in MCDB-131 medium containing hydrocortisone (1 µg/mL), epidermal growth factor (10 ng/mL), penicillin (50 unit/mL), streptomycin (50 unit/mL), L-glutamine (10 mM), and supplemented with 10% fetal bovine serum (FBS). At 90% confluence, before each treatment, cells were cultured overnight in serum-free medium. Chemicals were prepared as stock solutions in DMSO. The final concentration of vehicle did not exceed 0.2% (v/v); control cultures received the same concentration of DMSO. In all experiments using chemical inhibitors, cells were pre-treated 1 hour prior to and during exposure.

2.3. *Animal experimentation*

Long Evans rats (female of 180-200 g, Elevage Janvier, St Berthevin, France) were housed in plastic cages under controlled environment (12 h light/dark cycle, light on at 7 am, temperature of 22 ± 2°C

and relative humidity of 40 ± 5 %). Food and water were available *ad libitum*. The water, food and oil were tested according to NF ISO 15302 to confirm that all these matrices were PAH-free down to a detection limit of 10 ng/L of water and 1 ng/g of fat. Rats were acclimatized to the animal facility for 2 weeks prior to experiment onset. The mix of PAHs was composed of the 16 compounds pointed out the US-EPA for their toxicity, and prepared in vegetable oil weekly (ISIO4, Lesieur, Neuilly-sur-Seine, France). Treatment of animals has been described in a previous study[34]. Briefly, four rats were randomly allocated to each of the experimental group receiving 0.8 mg/kg body weight of each compound included in the mix, by oral administration, 3 times per week over a 90-day period. Control rats received only vehicle. At the end of 90 days-experiment, urine fractions were collected after 24 h in refrigerated tubes and storage at -20°C. All procedures were conducted in accordance with European Communities Council Directive of 22 September 2010 (2010/63/EU) and approved by the Ministry of Agriculture, Grand-Duchy of Luxembourg.

2.4. *Isolation of EVs from HMEC-1 cells*

Cells were cultured using cell culture petri dishes of 151.9 cm^2 (CorningTM, Thermo Fisher Scientific, France). After PAH exposure, in order to isolate total EVs, L-EV or S-EV, the serum-free conditioned medium was first centrifuged at 3650 x *g* for 10 min to remove cells and cell debris and obtain the cell-cleared supernatants. Total EVs were pelleted by direct ultracentrifugation of the culture media at 100,000 x *g* for 1h45 at 4°C (Beckman Coulter Optima L-90K Series Ultracentrifuges, rotor Sw 28.1); the pellet was then resuspended in sterile phosphate-buffered saline (PBS), followed by another centrifugation at 100,000 x *g* for 1h45 min at 4°C. Total EV pellets were finally resuspended in sterile PBS.

L-EVs were recovered from cell-cleared supernatants following centrifugation at 10 000 × *g* for 30 min, followed by one washing step in PBS at 10 000 × *g* for 30 min, and then resuspended in sterile PBS. S-EVs were further isolated from L-EVs-depleted supernatants following filtration at 0.2 µm

and a 100 000 x g ultracentrifugation step for 1h45 at 4°C, followed by one washing step in PBS at 100 000 x *g* for 1h45, and then resuspended in sterile PBS.

2.5. *Isolation of urine EVs*

About 9 mL of urine were first diluted half in PBS and centrifuged at 300 x *g* for 10 min, then 2 000 x *g* for 10 min to remove cells and cell debris. EVs were pelleted by ultracentrifugation at 100 000 × *g* for 2 h at 4°C (Beckman Coulter Optima L-90K Series Ultracentrifuges, rotor Sw 28.1). The pellet was next resuspended in sterile PBS containing dithiothreitol (DTT; 200 mg/mL) at 37°C for 10 minutes in order to dissociate of uromodulin aggregates[35,36], and then resuspended in sterile PBS, followed by another centrifugation at 100 000 × *g* for 2h at 4°C. Total EV pellets were finally resuspended in sterile PBS.

2.6. *Nanoparticle tracking analysis*

EV samples were diluted in sterile PBS before nanoparticle tracking analysis (NTA). Size distribution and vesicle concentration were determined by NTA using a NanoSight LM14 (Malvern Instruments, Malvern, UK). A 405 nm laser beam is used to highlight the samples. Three 30 s captures per sample were recorded at 25°C. Videos were analysed using NanoSight NTA 3.1 software (Malvern, UK) using a detection threshold set to 3. The presented results correspond at least to an average from three videos for each of three independent samples of EVs, S-EVs and L-EVs. EV concentrations and distributions were then normalized to the cell count and expressed as number of EVs released per cell.

2.7. *Electron microscopy*

Transmission electron microscopy (TEM) was performed as described by Théry et al.[37]. Briefly, S-EVs and L-EVs were resuspended in 2% paraformaldehyde (PFA). Formvar-carbon coated copper grids (Agar Scientific, Stansted, UK) were placed on 5 µL S-EVs or L-EVs suspension for 20 min and washed

with PBS. Vesicles were fixed in 1% glutaraldehyde in PBS for 5 minutes. After washing with distilled water, grids were placed on a drop of uranyl-oxalate for 5 min and of ice-cold 2% methyl cellulose/ 4% uranyl acetate (1/9; v/v) for 10 min. EVs were visualized using a JEOL JEM-1400 transmission electron microscope (JEOL, Japan).

2.8. *Annexin V binding analysis*

Staining by Annexin V-phycoerythrin (annexin V-PE, BD PharmingenTM) has been used to detect phosphatidylserine at the L-EV surfaces. An analysis window was defined using beads (Megamix, Stago) of diameters 0.5 µm, 0.9 µm and 3 µm. To determine the Annexin V positivity, L-EVs were incubated with Annexin V-PE, counting beads (Flow-Count™ Fluorospheres, Beckman) and buffer (14 mM NaCl, 10 mM Hepes, 2.5 mM calcium). Labelling in the absence of calcium was used as negative control. L-EVs stained with annexin V-PE were then analyzed by a BD FACSCanto™ III cytometer. Data have been exported using BD FACSDiva TM software.

2.9. *Western Blotting*

Total cellular, S-EV and L-EV protein amounts were estimated by a BCA Protein Assay Kit (Thermo Fisher Scientific, UK), using BSA as a standard. 5 µg proteins were separated by sodium dodecyl sulfate–polymerase gel electrophoresis (SDS–PAGE), and electrophoretically transferred onto nitrocellulose membranes (Merck Millipore). After blocking with a Tris-buffered saline solution supplemented with 2% bovine serum albumin for 2 h, membranes were hybridized with primary antibodies overnight at 4°C. Membranes were then incubated with horseradish peroxidase-conjugated secondary antibodies for 1 h. Immunolabeled proteins were visualized by chemiluminescence using the LAS-3000 analyzer (Fujifilm) or Molecular Imager ChemiDoc^{TM} XRS+ (Bio-Rad). Image processing was performed using Multi Gauge software (Fujifilm) or Image Lab^{TM} software (Bio-Rad). For protein loading evaluation, a primary antibody against HSC70 was used.

2.10. *Intracellular Calcium Concentration Measurements*

Cells used for intracellular calcium concentration ($[Ca^{2+}]_i$) measurements were grown on glass coverslips. The glass coverslips were sterilized in ethanol of increasing concentrations from 70 to 99%, and then coated with serum proteins using pure FBS prior to cell culture. Variations in $[Ca^{2+}]_i$ were analyzed in PAH-exposed HMEC-1 cells by real time fluorescence imaging, using Ca^{2+}-sensitive probe Fura-2-AM, as previously reported[25,38]. Briefly, cells were incubated at 37°C (30 min) in cell suspension buffer supplemented with 1.5 µM Fura-2AM and 0.006% pluronic acid. Changes in $[Ca^{2+}]_i$ were monitored using a DMIRB (Leica, Wetzlar, Germany) inverted microscope-based imaging system equipped with a 40×/1.35 UApo N340 high UV light transmittance oil immersion objective (Olympus, Waltham, MA, USA), a CoolSnapHQ fast-cooled monochromatic digital camera (Princeton instrument), a DG-4 Ultra High Speed Wavelength Switcher (Sutter Instruments, Novato, CA, USA) for fluorophore excitation, and METAFLUOR software (Universal Imaging, Downingtown, PA, USA) for image acquisition and analysis. The $[Ca^{2+}]_i$ imaging involved data acquisition every 10 s (emission at 510 nm) at 340- and 380-nm excitation wavelengths. The ratio of fluorescence intensities recorded after excitation at 340 nm (F340) and 380 nm (F380) was used to estimate intracellular calcium concentrations. $[Ca^{2+}]_i$ data were expressed as normalized maximum delta ratio, i.e., the difference between the basal level of $[Ca^{2+}]_i$ – related fluorescence ratios (F340/F380) before DMSO or PAH treatment and the maximum level of $[Ca^{2+}]_i$ – related fluorescence ratios (F340/F380) obtained during DMSO or PAH treatment.

2.11. *Apoptosis*

Cells used for apoptosis analysis were cultivated in 6-well plates. Hoechst 33342/Sytox green staining was carried out to observe apoptotic cells by fluorescence microscopy. After PAH exposure, cells were stained with 50 µg/mL Hoechst 33342 and 93.5 nM Sytox green in the dark at 37°C for 30 min. More than 300 cells in randomly selected microscopic fields were analyzed and were scored

under ZEISS Axio Scope A1 microscope. Cells with condensed or fragmented chromatin were counted as apoptotic.

2.12. *RNA Isolation and Analysis*

Total RNA was isolated from cells using the TRIzol® reagent (Invitrogen, Cergy Pontoise, France) and then reverse-transcribed using the High-Capacity cDNA Reverse Transcription Kit (Life Technologies, Carlsbad, CA, USA). Real-time quantitative PCR (RT-PCR) was performed using SYBR Green PCR Master Mix on the CFX384 Touch™ Real-Time PCR Detection System (Bio-Rad, Hercules, CA, USA). The mRNA expressions were normalized by means of 18s mRNA levels. The $2^{-\Delta\Delta ct}$ method was used to express the relative expression of each selected gene. Primers were as follows: CYP1A1-forwards: 5'- CCCACAGCACAACAAGAGACA-3'; CYP1A1-reverse: 5'-CATCAGGGGTGAGAAACCGT-3'; CYP1B1-forwards: 5'-AGCCAGGACACCCTTTCC-3'; CYP1B1-reverse: 5'-GAGTTGGACCAGGTTGTG-3'; 18S-forwards: 5'-CGCCGCTAGAGGTGAAATTC-3'; 18S-reverse: 5'-TTGGCAAATGCTTTCGCTC-3'.

2.13. *Statistical analysis*

All values were presented as means ± SEM from at least 3 independent experiments. Statistical analysis was performed using Student's *t* test and the one-way ANOVA with Dunnett's post hoc test (GraphPad Prism5, GraphPad Software, Inc, San Diego, California, USA). Significance was accepted at $p < 0.05$.

3. Results

3.1. B[a]P stimulates the production of EVs by endothelial HMEC-1 cells.

Endothelial cells constitute a well-known target for PAHs[25,39], and are part of the cells mainly producing EVs under physiological conditions[30]. We therefore decided to explore effects of B[a]P on EV production by the endothelial HMEC-1 cells using different concentrations and times of treatment. NTA revealed that B[a]P significantly stimulated EV production by HMEC-1 cells from 100 nM (Fig.1A) and after 12h of treatment (Fig.1B). After 24h of treatment with 100 nM B[a]P, observation by NTA of the size distribution profile of EVs (Fig.1C) showed that they exhibited diameters ranging from 50 nm to 600 nm, and that B[a]P stimulated the production of the entire population of EVs (regardless of EV size).

3.2. B[a]P stimulates the production of both S-EVs and L-EVs by endothelial HMEC-1 cells

It is known that cells can release an heterogeneous population of vesicles with variable diameters and different biogenesis processes, including small EVs (i.e. exosomes) formed inside endosomal compartments and larger EVs (i.e. microvesicles) budding from the plasma membrane. To get more insight into the characterization of the EV overproduction in treated HMEC-1 cells, we next evaluated the B[a]P effect by looking at both small (diameter <200 nm) and large (diameter >200 nm) EVs, following differential ultracentrifugation and filtration through 0.22 µm filters. Thus, our experimental procedure allowed us to isolate two populations of EVs: the small EV population (S-EVs) corresponding to EVs with average diameter of 160.1 ± 12.6 nm, and the large EV population (L-EVs) corresponding to EVs with average diameter of 295.8 ± 13.2 nm. Whereas B[a]P exposure (100 nM, 24h) did not change EV diameters (Fig. S1), it nonetheless increased the production of both S-EVs and L-EVs (Fig. 2A and 2B respectively), to the same extent (by about 2 fold) as for total EVs (Fig.1B).

3.3. S-EV and L-EV populations isolated from HMEC-1 cells correspond respectively to exosomes and microvesicles

In order to test whether S-EVs and L-EVs isolated under our experimental conditions correspond respectively to exosomes or microvesicles, we next examined their morphology and composition. As expected, TEM images revealed structures with expected cup-shaped appearance and diameters (Fig. 3A). By western blotting (Fig. 3B), using total cell lysates as positive controls, we failed to detect any lamin A/C in isolated S-EVs and L-EVs, thus ruling out a possible contamination of our EV samples by nucleus material. In contrast, proteins traditionally observed in both exosomes and microvesicles such as caveolin-1, flotillin-1, β-actin, Tsg101 and HSC70 (used as loading control), were detected in both S-EVs and L-EVs. Finally, a protein described to be more specific to exosome, that is CD63, was only detected in S-EVs (Fig. 3B) and cell lysates. It is known that microvesicles expose phosphatidylserine on their outer leaflet of the membrane[40,41]; therefore we next used the fluorescently labeled annexin V to analyze its presence in L-EVs (Fig. 3C). By flow cytometry, we found that 69 ± 3.6 % of isolated L-EVs were annexin-V positive.

Altogether, these observations indicated that our technical procedure allowed the isolation of S-EVs and L-EVs corresponding respectively to exosome- and microvesicle-enriched populations produced by HMEC-1 cells.

3.4. B[a]P would modify the protein cargoes of EVs produced by HMEC-1

In parallel to the characterization of S-EVs et L-EVs produced by HMEC-1 cells, we also investigated whether the EV composition and characteristics studied were affected by B[a]P exposure. At first, we found that no significant modification was observed in presence of B[a]P when looking at EV morphologies (Fig. 3A) or annexin V labeling (Fig. 3C). To analyze the protein cargoes of EVs, 5 µg of total proteins were subjected to SDS-PAGE western blotting to compare protein composition of S-EV or L-EVs produced by cells in presence or not of B[a]P (Fig. 3B). Cell lysates were used as positive control. Among the studied proteins, the levels of caveolin-1, flotillin-1 or β-actin appeared to be increased in EVs produced upon B[a]P exposure, especially in S-EVs. The densitometric analysis thus

revealed that caveolin-1 and flotillin-1 inductions were significant in the presence of this PAH (Fig.S2).

3.5. The increased production of S-EVs, but not L-EVs, upon B[a]P exposure would be AhR-dependent and calcium-independent

PAHs are known to trigger numerous interconnected cellular phenomena, associated or not to AhR activation, among them the induction of xenobiotic-metabolism enzymes, intracellular calcium signaling, membrane remodeling or apoptotic signaling[5,42,43]. Interestingly, several of them are also implicated in the production of EVs by cells. Thus, upon cell activation or apoptosis, the increase of $[Ca^{2+}]_i$ underlies the initiation of cell signaling pathways, remodeling of cytoskeleton and the redistribution of membrane phospholipids associated to the intracellular processing for exosome and/or microvesicles release[44]. To get further insight into the possible mechanisms involved in the EV production upon B[a]P exposure, we decided to focus our attention on AhR activation, calcium signal and apoptosis.

***Only AhR ligands can increase EV production by HMEC-1 cells*.** In order to test the possible involvement of AhR, we first decided to evaluate the potential of several PAHs with different AhR affinities, to increase EV production in HMEC-1 cells. To this aim, benzo[e]pyrene (B[e]P), pyrene (PYR), benz[a]anthracene (B[a]A) and dibenzo[a,h]anthracene (DBA) were chosen because they are part of the 16 U.S EPA priority pollutant PAH compounds; they are present in diet and possess different levels of affinity for AhR, therefore resulting in different potencies in terms of genomic AhR activation as compared to B[a]P (Fig. S3). The amount and size distribution of EVs produced by HMEC-1 cells were thus studied after 24 h of treatment with 100 nM of each PAH. Before focusing on EVs, we first evaluated the potential for AhR activation of our PAHs by studying the induction of known AhR-target genes, i.e. CYP1A1 and 1B1 (Fig. 4A). As expected, only B[a]A, B[a]P, and DBA (AhR ligands) induced CYP1A1 and 1B1 mRNA levels. The other PAHs tested (B[e]P and PYR), known to exhibit a very low affinity for AhR, failed to modify the expression of CYP1A1 and 1B1 in our cell

model. Interestingly, like B[a]P, B[a]A and DBA were both capable of increasing the EV production by HMEC-1 cells in contrast to B[e]P and PYR which were ineffective (Fig. 4B). Note that, whatever the PAH tested, analysis of the size distribution profile of EVs (Fig. 4C-F) indicated that isolated EVs had diameters ranging from 50 to 600 nm and that, when PAHs exhibited an effect on EV production, this concerned the entire population of EVs (whatever the size of EVs) (Fig.4E, 4F). To determine if a higher concentration of PAHs with low affinity for AhR was able to stimulate EV production by HMEC-1 cells, we decided to expose cells to 1 µM of PYR for 24h. Even at this high concentration, PYR failed to modify the EV production by HMEC-1 cells (Fig. S4A). This result thus confirms our data with 100 nM, and is concordant with recent publication from our group[45]. Indeed, we have recently demonstrated that PYR was able to increase S-EV production by hepatocytes independently of AhR, and through a Constitutive Androstane Receptor (CAR)-dependent mechanism. Interestingly, unlike hepatocytes, mRNAs of CAR were not detected in HMEC-1 cells (Fig. S4B).

An AhR antagonist (alpha-naphthoflavone) inhibits the production of S-EVs but not that of L-EVs induced by B[a]P. It is noteworthy that the PAH capacity to increase the mRNA levels of CYP1A1 and 1B1 dovetail with their capacity to increase the EV production by HMEC-1 cells. These observations led us to hypothesize an implication of AhR in the increased EV production upon B[a]P exposure. To test this hypothesis, we next investigated the effects of α-NF (antagonist of AhR and inhibitor of CYP1) on the B[a]P-triggered induction of S-EVs or L-EVs. As shown in Fig. 5, α-NF (10 µM) counteracted the up-regulation of S-EVs observed in presence of B[a]P (Fig.5A), while it failed to reduce the L-EV production (Fig. 5B). Interestingly, treatment by 6-formylindolo[3,2-b]carbazole (FICZ, 100 nM, 24h), a potent high affinity ligand of AhR, further supported this finding. Indeed, FICZ was able to increase the production of S-EVs but not that of L-EVs (Fig. S5). Therefore, AhR activation would be involved in the B[a]P-induced production of S-EVs but not of L-EVs, thus suggesting differential mechanisms.

PAH capacities to induce intracellular calcium concentration do not overlap their capacities to induce EV production. Knowing that calcium can be involved in EV production[18,44] and that B[a]P can increase $[Ca^{2+}]_i$ in HMEC-1 cells[25], we next decided to monitor the early $[Ca^{2+}]_i$ changes in response to our test PAHs. To do so, we used a real-time-fluorescence imaging method and the calcium-sensitive probe Fura2-AM. As previously described[25], B[a]P (100 nM) was able to increase $[Ca^{2+}]_i$ in HMEC-1 cells (Fig. 6A). The maximum of increase occurred after about 20 min of exposure to B[a]P (Fig. S6). We then analyzed the effects of 100 nM of all other tested PAHs, on $[Ca^{2+}]_i$ in order to determine the maximum level of $[Ca^{2+}]_i$ increase upon exposure to each molecule. Except for DBA, despite differences in terms of kinetics (Fig. S6), all PAHs were able to increase $[Ca^{2+}]_i$ in HMEC-1 cells, to the same extent as B[a]P (Fig. 6A). It is noteworthy that there was no correlation between PAH capacities to elevate $[Ca^{2+}]_i$ and those to increase EV production (Fig. 4B). Thus, B[e]P and PYR were found to induce $[Ca^{2+}]_i$ but failed to modify EV production by HMEC-1 cells; DBA stimulates EV production but did not modify $[Ca^{2+}]_i$; and B[a]P or B[a]A induced both $[Ca^{2+}]_i$ and EV production. Therefore, the early calcium signal triggered by PAHs would likely not be involved in the increased EV production, whatever the type of EVs considered.

PAH capacities to induce apoptosis do not overlap their capacities to induce EV production. As induction of CYP1A1 et 1B1 following AhR activation by PAHs could lead to apoptotic signaling[46], we then decided to evaluate apoptosis following PAH exposures (100 nM, 24 h). This was performed using fluorescence microscopy and Hoechst/Sytox green staining (Fig.6B). Consistent with literature, 100 nM B[a]P slightly (around 5%) but significantly increased the percentage of apoptotic cells. In contrast, the other tested PAHs, i.e. B[e]P, PYR, B[a]A and DBA, did not affect the apoptosis level. As for $[Ca^{2+}]_i$ induction, we therefore noted that there was no correlation between PAH capacities to induce apoptosis and PAH capacities to increase EV production by HMEC-1 cells.

3.6. *In vivo* exposure to a mixture of PAHs increases urinary EV amount

EVs are widely found in all body fluids including blood, saliva or urine[44]. Urine appears as non-invasive source for information reflecting the physio-pathological state of urinary system but also of other physiological systems. Based upon the fact that endothelial cells are part of kidney intrinsic cells producing urinary EVs (uEVs) and that humans are widely exposed to PAH mixture, we finally decided to test the *in vivo* effect of a mixture of the 16 PAHs listed as "priority" compounds by US-EPA, on the amount of EVs in rat urine samples. Thus, we evaluated uEVs amounts in urines collected during 24 h from rats exposed through diet for 90 days to 0.8 mg/kg of PAH mixture in comparison to control rats receiving only vehicle (vegetal oil). After isolation, uEV amounts were analyzed by NTA. As shown in Fig. 7A, rat exposure to PAH mixture led to an increase of uEVs number ($2.39.10^9$/mL *vs* $1.30.10^9$/mL) without any significant modification of renal functions, as determined by measuring urinary creatinine concentration and urinary volume (Fig. 7B and C).

4. Discussion

The growing interest for EVs originates (1)-from works demonstrating that EVs carry a plethora of bioactive molecules (i.e. nucleic acid, lipids, carbohydrates, proteins...) that play roles in cell-to-cell communication, and (2)-from works revealing the clinical interest of EVs as non-invasive diagnostic biomarkers in some human pathologies including cancer[47]. In this context, our study was performed in order to evaluate the capacity of PAHs to increase EV production both *in vitro* and *in vivo* with the aim of determining if these entities could represent potential biomarkers of exposure and/or effects of PAHs.

The present study highlights for the first time the capacity of PAHs to increase *in vitro* the EV production by endothelial HMEC-1 cells. Interestingly, only PAH ligands for AhR (i.e. B[a]P, B[a]A, DBA) led to this EV overproduction. Indeed, B[e]P and PYR, that are known weak AhR ligands, failed to modify such a production. Besides AhR activation, several PAHs can induce an intracellular calcium signaling[25] and trigger apoptosis[26], two cellular phenomena previously related to EV biogenesis[23,24]. Regarding influence of B[e]P, PYR, B[a]P, B[a]A, or DBA on intracellular calcium concentration, cell apoptosis and CYP1A1/1B1 mRNA levels, our results do support an AhR implication. Indeed, in contrast to the capacities to trigger an early $[Ca^{2+}]_i$ increase (as observed in presence of B[e]P, PYR, B[a]P, B[a]A) and apoptosis (as observed only in presence of B[a]P), the PAH capacity to induce mRNA levels of CY1A1 and 1B1 overlaps that to increase the EV production. These metabolism enzymes are well recognized as being under AhR control[5] and key actors in B[a]P induced apoptosis[26], and, like EVs, are induced in our cell model only by strong AhR ligands. Interestingly, only the increase of S-EV production was significantly counteracted by α–NF (AhR antagonist and inhibitor of CYP1), thus indicating that only the S-EV overproduction by B[a]P-treated HMEC-1 cells would be AhR dependent. These results therefore strengthen the fact that S-EV and L-EV biogenesis processes would differ, as previously proposed by other groups[48]It remains to determine the precise role for AhR in the S-EV production by HMEC-1 cells, notably in presence of

B[a]P. Many hypotheses could be considered. Thus, a possible involvement of the sphingolipid pathway would be particularly interesting to evaluate since, in epithelial cells, several AhR ligands, including PAHs, are able to promote the generation of sphingosine-1-phosphate, a bioactive intermediate of sphingolipid metabolism[49,50]. Indeed, sphingolipids and the enzymes related to their biosynthesis have been associated to EV biogenesis and release, especially by shaping membrane curvature[51]. Another hypothesis might involve a change in the physicochemical characteristics of lipid raft microdomains. Indeed, these entities, that are detected in EV membranes[23], represent assemblies of proteins and lipids within the plasma membrane that are notably enriched in cholesterol and sphingolipids[40]; most interestingly, they are elements of the regulatory mechanisms associated to the vesicle formation and structure[23]. As we have previously demonstrated that B[a]P alters the composition of the plasma membrane lipid microdomains notably through AhR activation[26], it could be interesting to test a role for such a membrane remodeling in the production of S-EVs by Hmec-1 cells. Of note, the present results indicate that B[a]P exposure could modify EV protein cargoes, notably leading to an enrichment of caveolin-1 and flotillin-1 contents in S-EVs. Interestingly, caveolin-1 and flotillin-1 are well-known markers of lipid rafts. Although studies of greater extent (i.e. proteomics) are needed to conclude, besides stimulating EV production, it seems that PAHs would moreover be able to modify the messages carried by the vesicles by modifying the composition of EVs.

Stimulating effects of PAHs, and more particularly B[a]P, towards EV production, concern the two main populations, namely S-EVs and L-EVs, as demonstrated by our EV characterization. As described in the literature, L-EV population (presently observed whatever the treatment applied), is relatively heterogonous as compared to the S-EV population. Looking only at their amount, L-EVs represent less than 20% of total EVs produced by HMEC-1 cells, whereas S-EVs represent more than 50%. Note that B[a]P treatment did not significantly affect this distribution (data not shown). Thus in terms of amount, S-EVs would represent the main type of EVs produced by HMEC-1 cells.

Nevertheless, considering averaged diameters (160 nm versus 300 nm for S-EVs and L-EVs respectively) and the corresponding averaged membrane surface area (0.08 μm^2 and 0.28 μm^2 for S-EVs and L-EVs respectively), it seems that L-EVs would not be a marginal population considering all EVs produced by HMEC-1. Since PAHs are environmental contaminants with numerous toxic effects on human cells, it could be interesting to determine if the observed L-EV overproduction is an attempt of exposed cells to remove B[a]P. Indeed, the microvesicle trafficking has been previously proposed as a biological process that helps cells to extrude potentially toxic xenobiotics[52], thus affording them a means of protection against an intracellular stress. This phenomenon is notably exploited by cancers cells as a mechanism of resistance. Indeed, microvesicles released from cancer cells, after drug treatment (i.e. doxorubicin), contain high levels of the chemotherapeutic agent[53]. Regarding the mechanisms involved in L-EV biogenesis upon B[a]P exposure, they yet remain to be determined. However, it seems that neither early calcium signal triggered by PAHs, neither AhR would be involved in their production.

Regarding the effects, notably carcinogenic, of PAHs on human health, the monitoring of the populations likely exposed to these pollutants is currently performed through the measurement of urinary PAH metabolites (i.e. 1-hydroxy pyrene, 3-hydroxy B[a]P), or by evaluation of DNA-adducts in blood cells[54]. The use of these biomarkers is difficult since their presence does not necessarily reflect the level of PAH mixture humans are exposed to [54]. Moreover, these biomarkers are related to the capacity of cells to metabolize PAHs but not to the cellular reaction towards these pollutants. Considering these aspects, it therefore seems that studying EVs in body fluids as urine would be a good alternative. Indeed, EV production can be correlated to cellular response, to disease, to drug exposure[18]. Our present results indicate that B[a]P, B[a]A and DBA are each able to up-regulate production of EVs from endothelial cells. This induction effect was also observed *in vivo* upon exposure to a mixture of PAHs. Thus, our data show that rat exposure (90 days) to the mixture of 16 US-EPA PAHs, was capable of increasing the EV disposal from urine without influencing renal

activity. These results therefore suggest that EVs in urine may have particular utility for monitoring exposure to toxicants and to detect the related early cellular response prior to end-organ damages.

5. Conclusion

Taken together, our data indicates that, i) PAH exposure increases *in vitro* the EV production by endothelial cells and *in vivo* the release of EVs in urine, and that the stimulating effects of PAHs concern both S-EVs (or exosomes) and L-EVs (or microvesicles); ii) PAH exposure and more particularly, exposure to B[a]P, might influence the composition of the S-EVs produced by endothelial cells; and finally, iii) AhR would be involved in the PAH effects on the release of S-EVs, but not L-EVs. The inability of AhR weak ligands, like PYR or B[e]P, to increase the EV production in HMEC-1 cells, along with the inhibitory effects of α–NF, an AhR antagonist, towards the B[a]P effect on the S-EV production strongly support this assumption. In total, our results therefore point to EVs as possibly useful biomarkers of exposure for PAHs.

References

1. Remoundou, K. & Koundouri, P. Environmental Effects on Public Health: An Economic Perspective. *Int. J. Environ. Res. Public. Health* **6**, 2160–2178 (2009).
2. Ferronato, N. & Torretta, V. Waste Mismanagement in Developing Countries: A Review of Global Issues. *Int. J. Environ. Res. Public. Health* **16**, 1060 (2019).
3. Bansal, V. & Kim, K.-H. Review of PAH contamination in food products and their health hazards. *Environ. Int.* **84**, 26–38 (2015).
4. Haarmann-Stemmann, T., Bothe, H. & Abel, J. Growth factors, cytokines and their receptors as downstream targets of arylhydrocarbon receptor (AhR) signaling pathways. *Biochem. Pharmacol.* **77**, 508–520 (2009).

5. Larigot, L., Juricek, L., Dairou, J. & Coumoul, X. AhR signaling pathways and regulatory functions. *Biochim. Open* **7**, 1–9 (2018).
6. Bruzzoniti, M. C., Fungi, M. & Sarzanini, C. Determination of EPA's priority pollutant polycyclic aromatic hydrocarbons in drinking waters by solid phase extraction-HPLC. *Anal. Methods* **2**, 739 (2010).
7. Benedikter, B. J., Wouters, E. F. M., Savelkoul, P. H. M., Rohde, G. G. U. & Stassen, F. R. M. Extracellular vesicles released in response to respiratory exposures: implications for chronic disease. *J. Toxicol. Environ. Health Part B* **21**, 142–160 (2018).
8. Conde-Vancells, J., Gonzalez, E., Lu, S. C., Mato, J. M. & Falcon-Perez, J. M. Overview of extracellular microvesicles in drug metabolism. *Expert Opin. Drug Metab. Toxicol.* **6**, 543–554 (2010).
9. Rak, J. Extracellular Vesicles – Biomarkers and Effectors of the Cellular Interactome in Cancer. *Front. Pharmacol.* **4**, (2013).
10. Soekmadji, C. & Nelson, C. C. The Emerging Role of Extracellular Vesicle-Mediated Drug Resistance in Cancers: Implications in Advanced Prostate Cancer. *BioMed Res. Int.* **2015**, 1–13 (2015).
11. Wang, J. W. *et al.* Plasma extracellular vesicle protein content for diagnosis and prognosis of global cardiovascular disease. *Neth. Heart J.* **21**, 467–471 (2013).
12. Bebelman, M. P., Smit, M. J., Pegtel, D. M. & Baglio, S. R. Biogenesis and function of extracellular vesicles in cancer. *Pharmacol. Ther.* **188**, 1–11 (2018).
13. Maas, S. L. N., Breakefield, X. O. & Weaver, A. M. Extracellular Vesicles: Unique Intercellular Delivery Vehicles. *Trends Cell Biol.* **27**, 172–188 (2017).
14. Hartjes, T., Mytnyk, S., Jenster, G., van Steijn, V. & van Royen, M. Extracellular Vesicle Quantification and Characterization: Common Methods and Emerging Approaches. *Bioengineering* **6**, 7 (2019).

15. Bayraktar, R., Van Roosbroeck, K. & Calin, G. A. Cell-to-cell communication: microRNAs as hormones. *Mol. Oncol.* **11**, 1673–1686 (2017).
16. Jaiswal, R. & Sedger, L. M. Intercellular Vesicular Transfer by Exosomes, Microparticles and Oncosomes - Implications for Cancer Biology and Treatments. *Front. Oncol.* **9**, (2019).
17. Curtis, A. M. *et al.* Endothelial microparticles: Sophisticated vesicles modulating vascular function. *Vasc. Med.* **18**, 204–214 (2013).
18. Martínez, M. C. & Andriantsitohaina, R. Extracellular Vesicles in Metabolic Syndrome. *Circ. Res.* **120**, 1674–1686 (2017).
19. Bala, S. *et al.* Circulating microRNAs in exosomes indicate hepatocyte injury and inflammation in alcoholic, drug-induced, and inflammatory liver diseases. *Hepatology* **56**, 1946–1957 (2012).
20. Benedikter, B. J. *et al.* Cigarette smoke extract induced exosome release is mediated by depletion of exofacial thiols and can be inhibited by thiol-antioxidants. *Free Radic. Biol. Med.* **108**, 334–344 (2017).
21. Cesselli, D. *et al.* Extracellular Vesicles: How Drug and Pathology Interfere With Their Biogenesis and Function. *Front. Physiol.* **9**, (2018).
22. Palomo, L. *et al.* Abundance of Cytochromes in Hepatic Extracellular Vesicles Is Altered by Drugs Related With Drug-Induced Liver Injury. *Hepatol. Commun.* **2**, 1064–1079 (2018).
23. Pollet, H., Conrard, L., Cloos, A.-S. & Tyteca, D. Plasma Membrane Lipid Domains as Platforms for Vesicle Biogenesis and Shedding? *Biomolecules* **8**, 94 (2018).
24. Turturici, G., Tinnirello, R., Sconzo, G. & Geraci, F. Extracellular membrane vesicles as a mechanism of cell-to-cell communication: advantages and disadvantages. *Am. J. Physiol.-Cell Physiol.* **306**, C621–C633 (2014).
25. Mayati, A. *et al.* Induction of Intracellular Calcium Concentration by Environmental Benzo(*a*)pyrene Involves a β2-Adrenergic Receptor/Adenylyl Cyclase/Epac-1/Inositol 1,4,5-Trisphosphate Pathway in Endothelial Cells. *J. Biol. Chem.* **287**, 4041–4052 (2012).

567 26. Tekpli, X. *et al.* Membrane remodeling, an early event in benzo[α]pyrene-induced apoptosis.
568 *Toxicol. Appl. Pharmacol.* **243**, 68–76 (2010).
569 27. Pergoli, L. *et al.* Extracellular vesicle-packaged miRNA release after short-term exposure to
570 particulate matter is associated with increased coagulation. *Part. Fibre Toxicol.* **14**, (2017).
571 28. Ryu, A.-R., Kim, D. H., Kim, E. & Lee, M. Y. The Potential Roles of Extracellular Vesicles in
572 Cigarette Smoke-Associated Diseases. *Oxid. Med. Cell. Longev.* **2018**, 1–8 (2018).
573 29. Kranendonk, M. E. *et al.* Extracellular vesicle markers in relation to obesity and metabolic
574 complications in patients with manifest cardiovascular disease. *Cardiovasc. Diabetol.* **13**, 37
575 (2014).
576 30. Iba, T. & Ogura, H. Role of extracellular vesicles in the development of sepsis-induced
577 coagulopathy. *J. Intensive Care* **6**, (2018).
578 31. Barreiro, K. & Holthofer, H. Urinary extracellular vesicles. A promising shortcut to novel
579 biomarker discoveries. *Cell Tissue Res.* **369**, 217–227 (2017).
580 32. Lv, L.-L., Feng, Y., Tang, T.-T. & Liu, B.-C. New insight into the role of extracellular vesicles
581 in kidney disease. *J. Cell. Mol. Med.* **23**, 731–739 (2019).
582 33. Pisitkun, T., Shen, R.-F. & Knepper, M. A. Identification and proteomic profiling of exosomes
583 in human urine. *Proc. Natl. Acad. Sci.* **101**, 13368–13373 (2004).
584 34. Grova, N., Faÿs, F., Hardy, E. M. & Appenzeller, B. M. R. New insights into urine-based
585 assessment of polycyclic aromatic hydrocarbon-exposure from a rat model: Identification of
586 relevant metabolites and influence of elimination kinetics. *Environ. Pollut.* **228**, 484–495
587 (2017).
588 35. Fernández-Llama, P. *et al.* Tamm-Horsfall protein and urinary exosome isolation. *Kidney Int.*
589 **77**, 736–742 (2010).
590 36. Musante, L. *et al.* A Simplified Method to Recover Urinary Vesicles for Clinical Applications
591 and Sample Banking. *Sci. Rep.* **4**, 7532 (2015).

592 37. Théry, C., Amigorena, S., Raposo, G. & Clayton, A. Isolation and Characterization of
593 Exosomes from Cell Culture Supernatants and Biological Fluids. *Curr. Protoc. Cell Biol.* **30**,
594 3.22.1-3.22.29 (2006).
595 38. Brinchmann, B. *et al.* Lipophilic Chemicals from Diesel Exhaust Particles Trigger Calcium
596 Response in Human Endothelial Cells via Aryl Hydrocarbon Receptor Non-Genomic
597 Signalling. *Int. J. Mol. Sci.* **19**, 1429 (2018).
598 39. Brinchmann, B. C. *et al.* Lipophilic components of diesel exhaust particles induce pro-
599 inflammatory responses in human endothelial cells through AhR dependent pathway(s). *Part.*
600 *Fibre Toxicol.* **15**, 21 (2018).
601 40. Head, B. P., Patel, H. H. & Insel, P. A. Interaction of membrane/lipid rafts with the
602 cytoskeleton: Impact on signaling and function. *Biochim. Biophys. Acta BBA - Biomembr.* **1838**,
603 532–545 (2014).
604 41. Record, M., Silvente-Poirot, S., Poirot, M. & Wakelam, M. J. O. Extracellular vesicles: lipids as
605 key components of their biogenesis and functions. *J. Lipid Res.* **59**, 1316–1324 (2018).
606 42. Holme, J. A., Brinchmann, B. C., Le Ferrec, E., Lagadic-Gossmann, D. & Øvrevik, J.
607 Combustion Particle-Induced Changes in Calcium Homeostasis: A Contributing Factor to
608 Vascular Disease? *Cardiovasc. Toxicol.* **19**, 198–209 (2019).
609 43. Tekpli, X., Holme, J. A., Sergent, O. & Lagadic-Gossmann, D. Role for membrane remodeling
610 in cell death: Implication for health and disease. *Toxicology* **304**, 141–157 (2013).
611 44. Yáñez-Mó, M. *et al.* Biological properties of extracellular vesicles and their physiological
612 functions. *J. Extracell. Vesicles* **4**, 27066 (2015).
613 45. van Meteren, N. *et al.* Polycyclic aromatic hydrocarbons can trigger a hepatocyte release of
614 extracellular vesicles by various mechanisms of action depending on their affinity for aryl
615 hydrocarbon receptor. *Toxicol. Sci.* (2019). doi:10.1093/toxsci/kfz157

46. Hardonnière, K., Huc, L., Sergent, O., Holme, J. A. & Lagadic-Gossmann, D. Environmental carcinogenesis and pH homeostasis: Not only a matter of dysregulated metabolism. *Semin. Cancer Biol.* **43**, 49–65 (2017).
47. Nawaz, M., Fatima, F. & Squire, J. A. Mining Extracellular Vesicles for Clinically Relevant Noninvasive Diagnostic Biomarkers in Cancer. in *Novel Implications of Exosomes in Diagnosis and Treatment of Cancer and Infectious Diseases* (ed. Wang, J.) (InTech, 2017). doi:10.5772/intechopen.69406
48. Abels, E. R. & Breakefield, X. O. Introduction to Extracellular Vesicles: Biogenesis, RNA Cargo Selection, Content, Release, and Uptake. *Cell. Mol. Neurobiol.* **36**, 301–312 (2016).
49. Reiners, J. J. & Clift, R. E. Aryl Hydrocarbon Receptor Regulation of Ceramide-induced Apoptosis in Murine Hepatoma 1c1c7 Cells: a function independent of aryl hydrocarbon receptor nuclear translocator. *J. Biol. Chem.* **274**, 2502–2510 (1999).
50. Wang, H.-C. *et al.* Aryl hydrocarbon receptor signaling promotes ORMDL3-dependent generation of sphingosine-1-phosphate by inhibiting sphingosine-1-phosphate lyase. *Cell. Mol. Immunol.* (2018). doi:10.1038/s41423-018-0022-2
51. Verderio, C., Gabrielli, M. & Giussani, P. Role of sphingolipids in the biogenesis and biological activity of extracellular vesicles. *J. Lipid Res.* **59**, 1325–1340 (2018).
52. Jorfi, S. & Inal, J. M. The role of microvesicles in cancer progression and drug resistance. *Biochem. Soc. Trans.* **41**, 293–298 (2013).
53. Shedden, K., Xie, X. T., Chandaroy, P., Chang, Y. T. & Rosania, G. R. Expulsion of Small Molecules in Vesicles Shed by Cancer Cells: Association with Gene Expression and Chemosensitivity Profiles1,2. *Cancer Res* **63**, 4331–7 (2003).
54. Srogi, K. Monitoring of environmental exposure to polycyclic aromatic hydrocarbons: a review. *Environ. Chem. Lett.* **5**, 169–195 (2007).

Acknowledgements

We first wish to thank Dr Carmen Martinez (UMR Inserm 1063, Angers, France) for valuable discussion on EVs at the beginning of this project. We are also very grateful to the MRiC platform (UMS BIOSIT, Rennes, France), notably Stéphanie Dutertre for training us on calcium measurements. This study was financially supported by the “Programme Environnement-Santé-Travail” of Anses with the funding from ITMO cancer in the context of the Cancer Plan 2014-2019 (EST-2016/1/31), and by the Cancéropôle Grand-Ouest/Région Bretagne (Concerto project). Manon Le Goff was a recipient of a PhD fellowship from the Collectivités Locales Mayennaises.

650 **Figure legends**

651 **Figure 1. B[a]P stimulates the extracellular vesicle release from endothelial HMEC-1 cells.** Total
652 EVs were isolated by ultracentrifugation and analyzed by Nanoparticle Tracking Analysis (NTA). (**A**)
653 EVs released per HMEC-1 cells exposed to vehicle (DMSO) or 1 nM to 10 000 nM B[a]P for 24 h, and
654 (**B**) exposed to 100 nM B[a]P from 2 h to 24 h. (**C**) Size distribution profile by NTA of EVs produced
655 by endothelial cells during 24h at 100 nM B[a]P. Data are the means ± SEM of three or more
656 independent assays. *p < 0.05; **p < 0.01; ***p < 0.001 significantly different from unexposed
657 control.

658 **Figure 2. B[a]P stimulates the production of both small vesicles (S-EVs) and large (L-EVs) vesicles**
659 **from endothelial HMEC-1 cells.** HMEC-1 cells were exposed to vehicle (DMSO) or 100 nM B[a]P for
660 24 h. S-EVs and L-EVs were isolated by differential ultracentrifugation, as described in Material and
661 Methods section. Size distribution profile, determined by Nanoparticle Tracking Analysis (NTA) and
662 amount (inserts) of S-EVs (**A**) and L-EVs (**B**) released per endothelial cell. Data are the means ± SEM
663 of three or more independent assays. *p < 0.05; **p < 0.01 significantly different from unexposed
664 control.

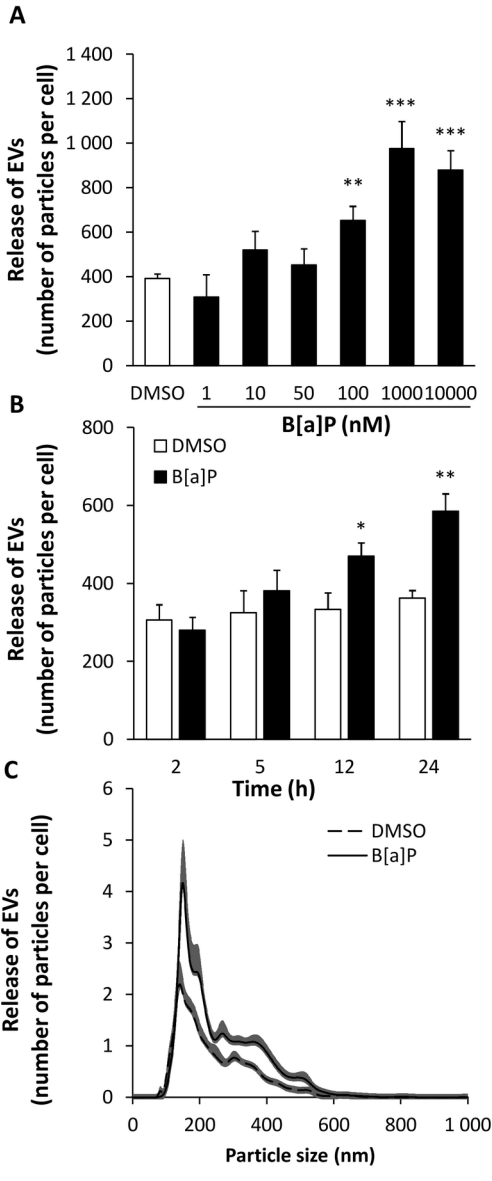
665 **Figure 3. Characterization of S-EV and L-EV populations isolated from endothelial HMEC-1 cells.**
666 HMEC-1 cells were exposed to vehicle (DMSO) or 100 nM B[a]P for 24 h. S-EVs and L-EVs were
667 isolated by differential ultracentrifugation, as described in Material and Methods section. (**A**)
668 Transmission electron microscopy pictures of S-EV and L-EV pellets (scale bars = 200 nm). (**B**)
669 Western blot analysis of EV markers in S-EVs and L-EVs obtained from HMEC-1. Cell lysates were
670 used as positive control for each marker studied. Lamin A/C was used to evaluate nuclear sample
671 contamination; caveolin-1, flotillin-1, TSG101and β-actin were used as markers of both S-EVs and L-
672 EVs. CD63 was used as S-EV specific markers, and Hsc70 was used as loading control. (**C**)
673 Measurement of annexin V positivity of L-EVs by flow cytometry. Annexin V was used as marker for
674 phosphatidylserine. Results are expressed as a percentage of isolated L-EVs.

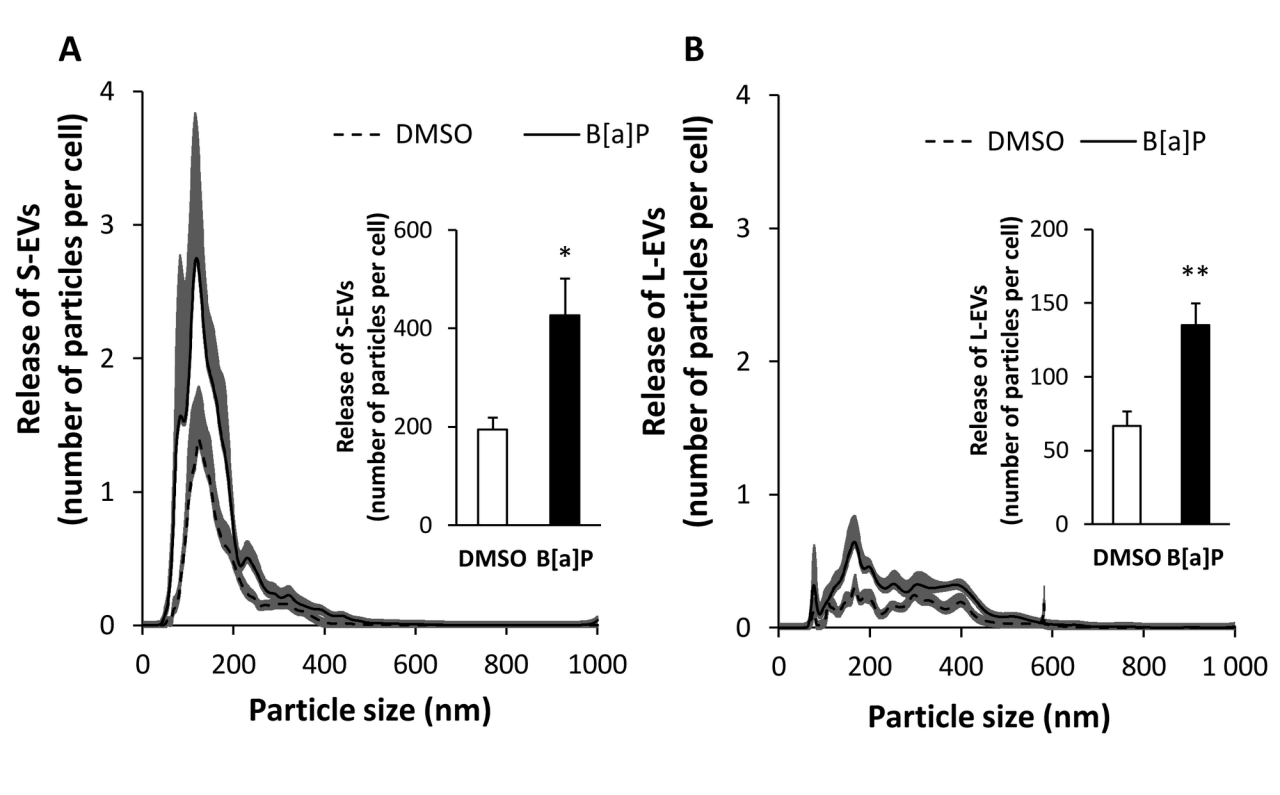
Figure 4. Effects of PAHs on the EVs released from endothelial HMEC-1 cells. (**A**-**F**) HMEC-1 cells were exposed to vehicle (DMSO) or 100 nM of B[e]P, PYR, B[A]A, B[a]P or DBA for 24 h. (**A**) mRNA expression of CYP1A1 and CYP1B1 was analyzed using RT-qPCR. Data are expressed relatively to mRNA levels of CYP1A1 and CYP1B1 found in corresponding control cells (DMSO), arbitrarily set to 1 unit. (**B**-**F**) Total EVs were isolated by ultracentrifugation and analyzed by Nanoparticle Tracking Analysis (NTA). (**B**) EV production released per HMEC-1 cells exposed to different PAHs for 24 h. (**C**-**F**) Size distribution profile by NTA of EVs produced by endothelial cells during a 24 h exposure with different PAHs compared to control (DMSO). Data are the means ± SEM of three or more independent assays. *p < 0.05; **p < 0.01; ***p < 0.001 significantly different from unexposed control.

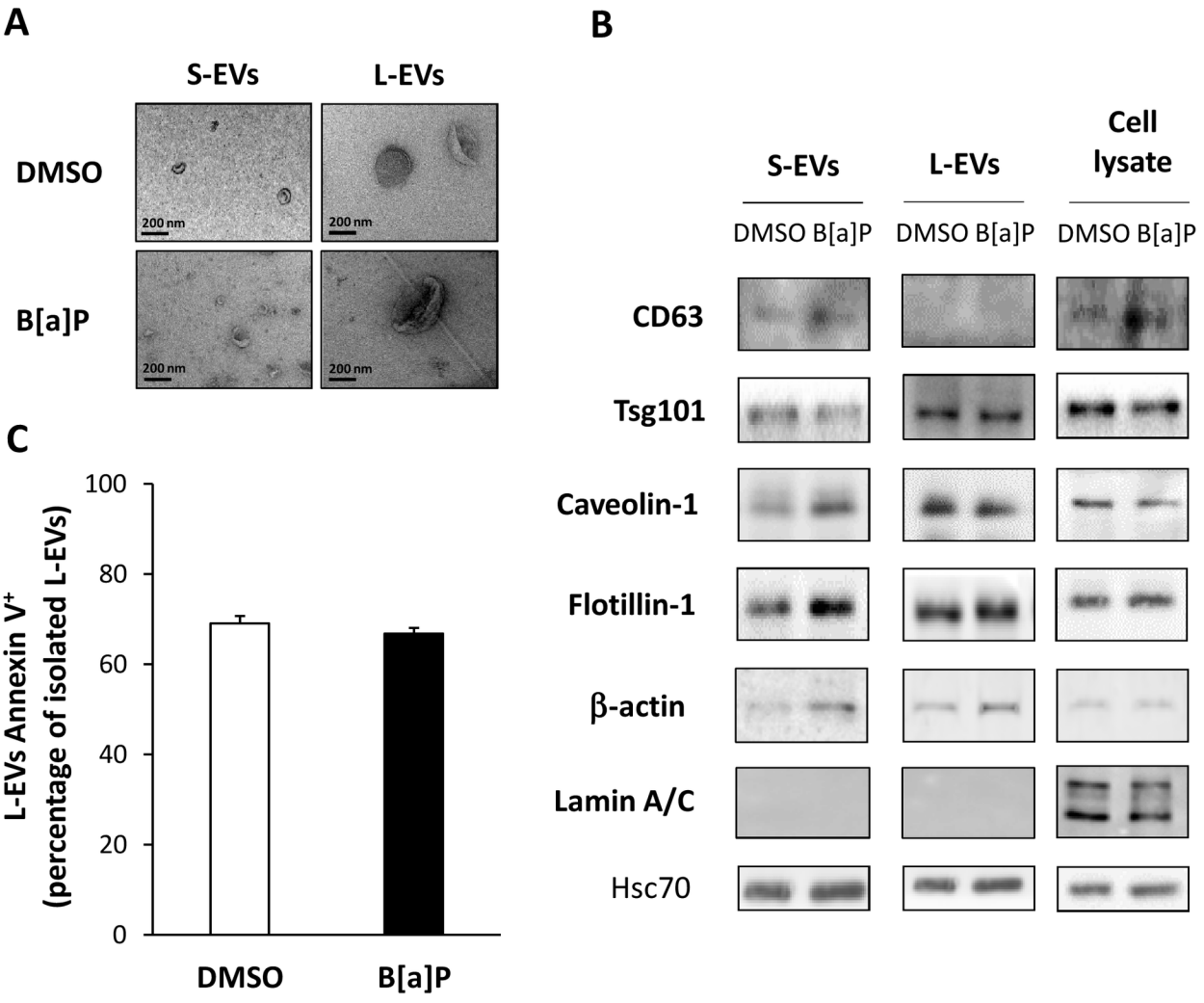
Figure 5: Involvement of AhR in the production of S-EVs, but not of L-EVs, produced upon B[a]P exposure of endothelial HMEC-1 cells. HMEC-1 cells were exposed to vehicle (DMSO) or 100 nM B[a]P in presence or not to AhR antagonist α-NF (10 µM). S-EVs and L-EVs were isolated by differential ultracentrifugation, as described in Material and Methods section. S-EV (**A**) and L-EV (**B**) concentrations released per endothelial cell were determined by Nanoparticle Tracking Analysis (NTA). Data are the means ± SEM of three or more independent assays. *p < 0.05 significantly different from unexposed control. $^{\#}$p < 0.05 significantly different from B[a]P-treated cells.

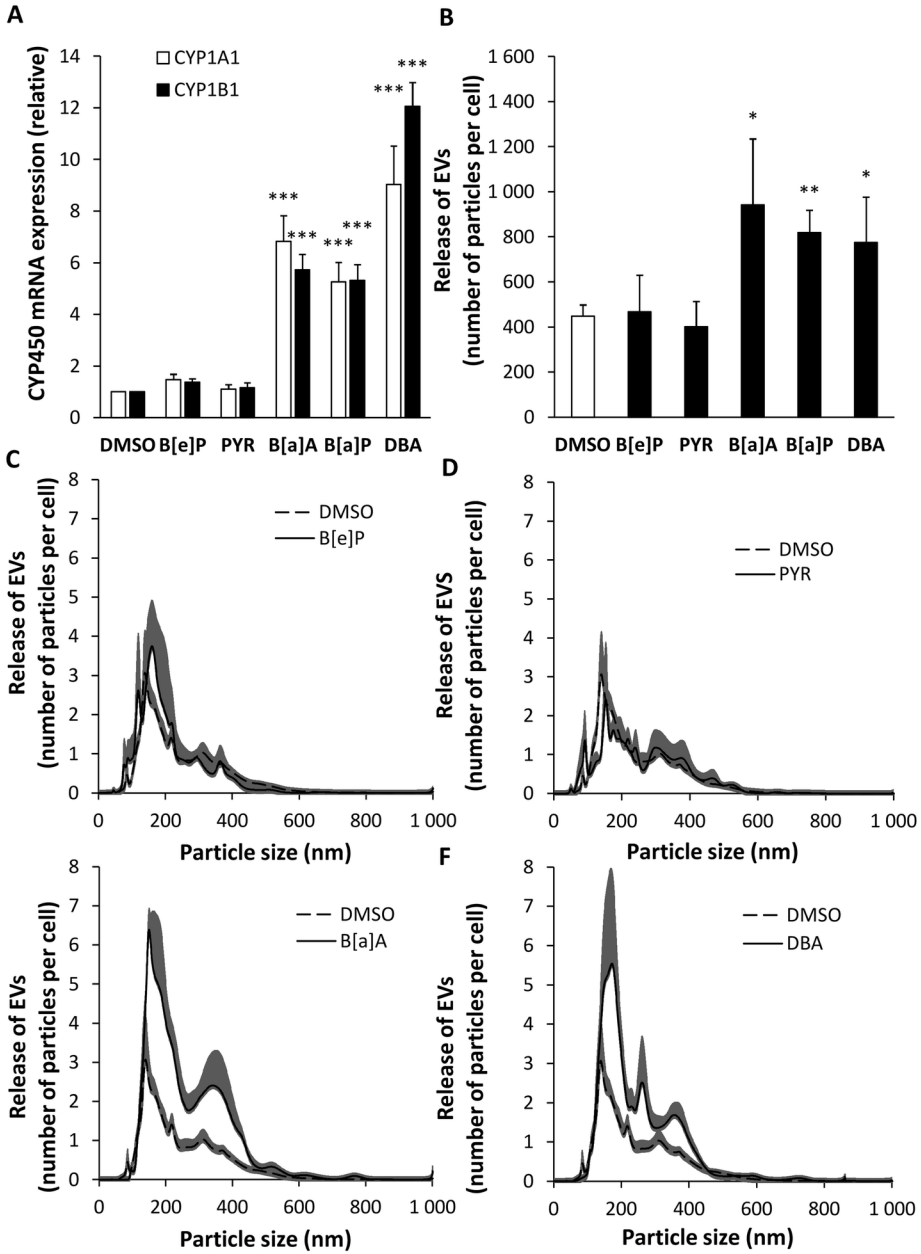
Figure 6. PAH effects on intracellular Ca^{2+} concentrations ($[Ca^{2+}]_i$) and on the apoptosis in HMEC-1 cells. HMEC-1 cells were exposed to vehicle (DMSO) or 100 nM of B[e]P, PYR, B[A]A, B[a]P or DBA. (**A**) $[Ca^{2+}]_i$ in cells was analyzed by real time fluorescence imaging, using Ca^{2+}-sensitive probe Fura2-AM (acetoxymethyl ester). Data were expressed as normalized maximum delta ratio as described in Materials and Methods. HMEC-1 cells were treated by B[e]P, PYR, B[A]A, B[a]P or DBA at 100 nM or untreated (DMSO) during 24 h for the evaluation of cytotoxicity by (**B**) counting apoptotic cells. Data are the means ± SEM of three or more independent assays. *p < 0.05; **p < 0.01; ***p < 0.001 significantly different from unexposed control.

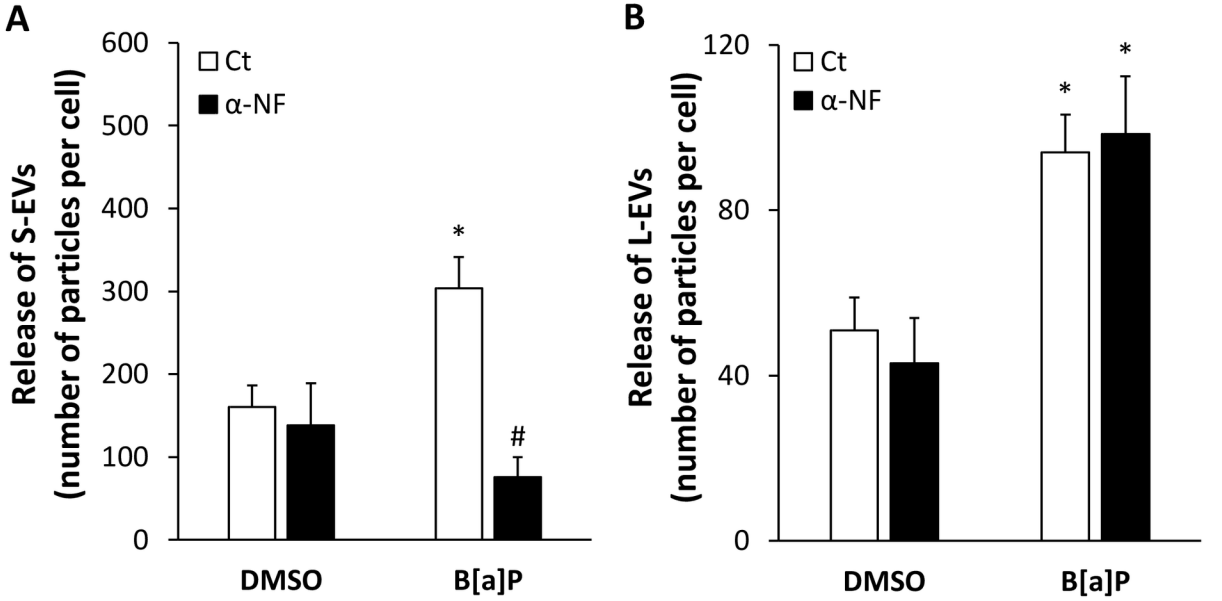
Figure 7. *In vivo* PAH exposure increases EV amount in urine. Rats received 0.8 mg/kg of a 16 PAH mixture or only vehicle for control rats during 90 days. At the end of 90 days-experiment, urine fractions were collected over a 24 h period. EVs were isolated by differential ultracentrifugation. (**A**) EV concentrations released per mL of urine were assessed by Nanoparticle Tracking Analysis. (**B**) Creatinine concentration (mg/mL) in urine of rats. (**C**) Urinary volume produced during the last 24 hours of PAH exposure. Data are the means ± SEM of four rats. ***$p < 0.001$ significantly different from unexposed control.

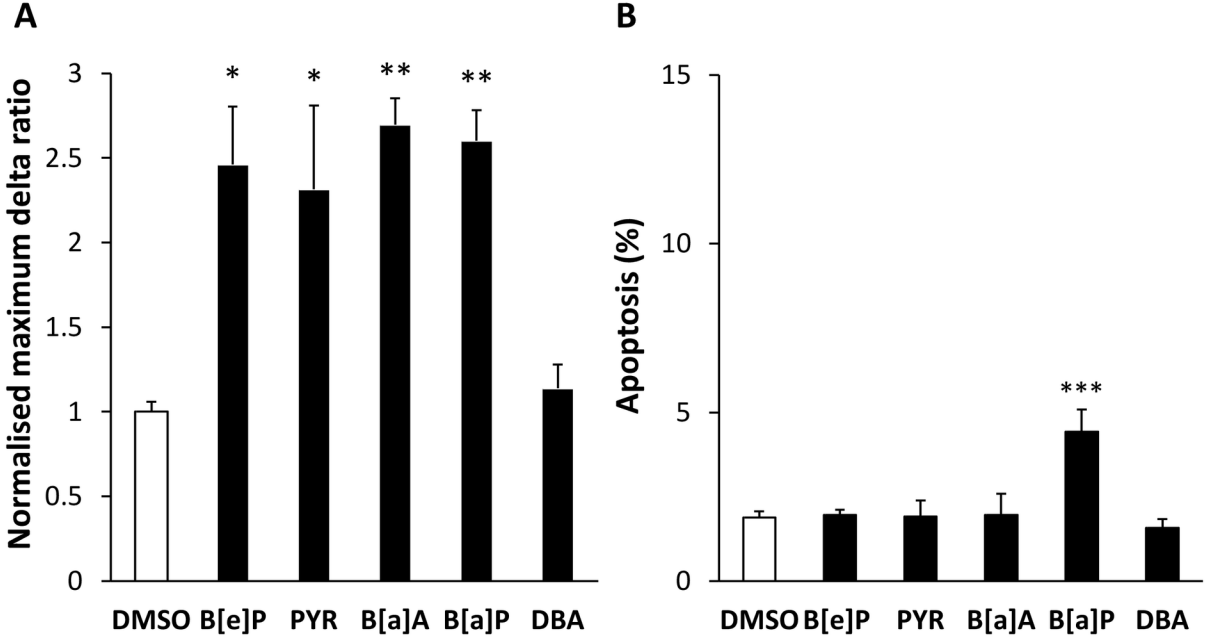

A
Release of EVs
(number of particles per cell)
1 400
1 200
1 000
800
600
400
200
0
**
***
***
DMSO
1
10
50
100
1000
10000
B[a]P (nM)
B
Release of EVs
(number of particles per cell)
800
600
400
200
0
DMSO
B[a]P
*
**
2
5
12
24
Time (h)
C
Release of EVs
(number of particles per cell)
6
5
4
3
2
1
0
DMSO
B[a]P
0
200
400
600
800
1 000
Particle size (nm)

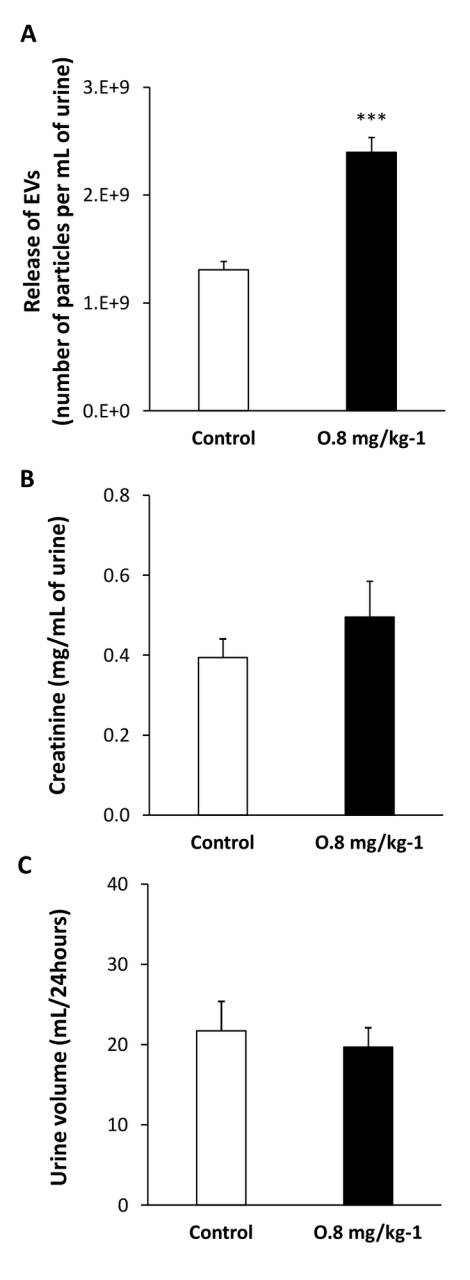

A
B
DMSO
B[a]P
Release of S-EVs (number of particles per cell)
Release of L-EVs (number of particles per cell)
Particle size (nm)
0
200
400
600
800
1000
1 000
1
2
3
4
50
100
150
*
**
DMSO B[a]P

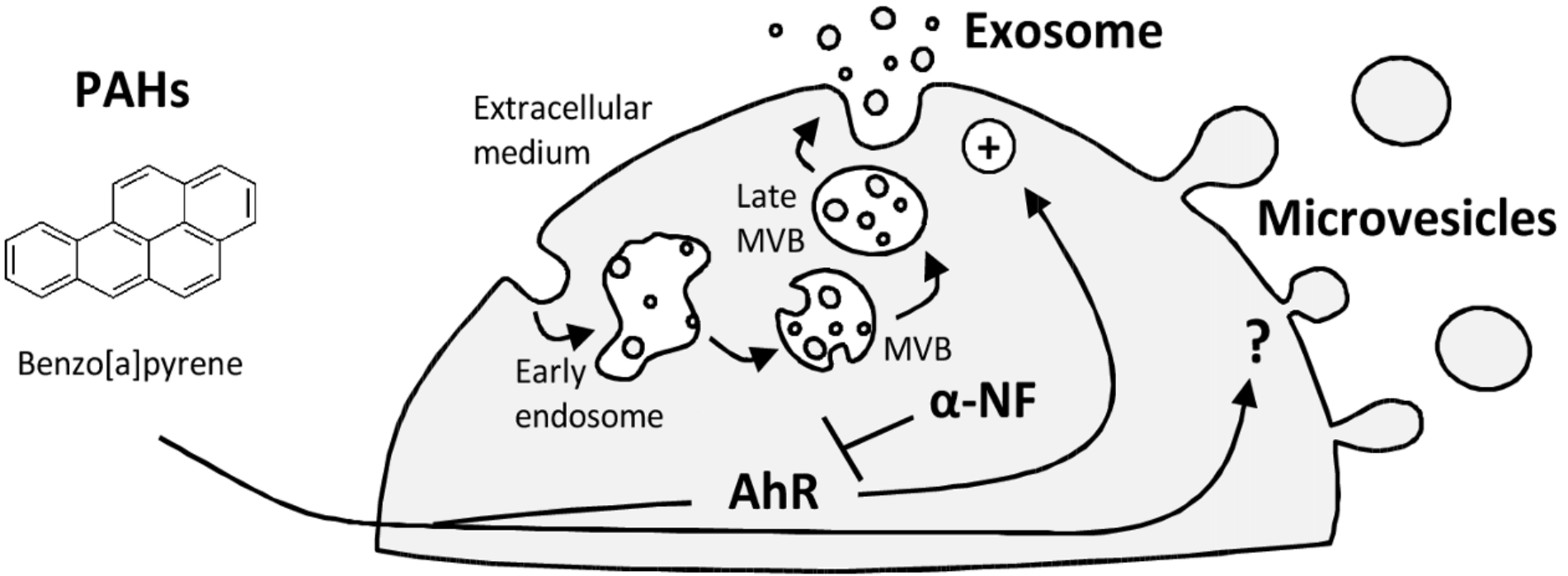

A
S-EVs
L-EVs
DMSO
B[a]P
200 nm
200 nm
200 nm
200 nm
B
S-EVs
L-EVs
Cell lysate
DMSO B[a]P
DMSO B[a]P
DMSO B[a]P
CD63
Tsg101
Caveolin-1
Flotillin-1
β-actin
Lamin A/C
Hsc70
C
L-EVs Annexin V+ (percentage of isolated L-EVs)
100
80
60
40
20
0
DMSO
B[a]P


A
CYP450 mRNA expression (relative)
CYP1A1
CYP1B1
DMSO B[e]P PYR B[a]A B[a]P DBA
B
Release of EVs (number of particles per cell)
DMSO B[e]P PYR B[a]A B[a]P DBA
C
Release of EVs (number of particles per cell)
DMSO
B[e]P
Particle size (nm)
D
Release of EVS (number of particles per cell)
DMSO
PYR
Particle size (nm)
E
Release of EVs (number of particles per cell)
DMSO
B[a]A
Particle size (nm)
F
Release of EVs (number of particles per cell)
DMSO
DBA
Particle size (nm)


A
Release of S-EVs
(number of particles per cell)
600
500
400
300
200
100
0
Ct
α-NF
*
#
DMSO
B[a]P
B
Release of L-EVs
(number of particles per cell)
120
80
40
0
Ct
α-NF
*
*
DMSO
B[a]P


A
Normalised maximum delta ratio
3
2.5
2
1.5
1
0.5
0
*
*
**
**
DMSO
B[e]P
PYR
B[a]A
B[a]P
DBA
B
Apoptosis (%)
15
10
5
0
***
DMSO
B[e]P
PYR
B[a]A
B[a]P
DBA


A
Release of EVs
(number of particles per mL of urine)
3.E+9
2.E+9
1.E+9
0.E+0
***
Control
O.8 mg/kg-1
B
Creatinine (mg/mL of urine)
0.8
0.6
0.4
0.2
0.0
Control
O.8 mg/kg-1
C
Urine volume (mL/24hours)
40
30
20
10
0
Control
O.8 mg/kg-1


PAHs
Benzo[a]pyrene
Extracellular medium
Exosome
Late MVB
MVB
Early endosome
α-NF
AhR
?
Microvesicles